의학박사 학위논문

Regional thickness of the skin and superficial fat in Asian faces

동양인의 얼굴 피부 및 얕은 얼굴지방의 부위별 두께

2019 년 8 월

서울대학교 대학원

의학과 해부학전공

김 유 수

A thesis of the Degree of Doctor of Philosophy

Regional thickness of the skin and superficial fat in Asian faces

동양인의 얼굴 피부 및 얕은 얼굴지방의 부위별 두께

August, 2019

Department of Anatomy

Graduate School of Medicine

Seoul National University

You Soo Kim

동양인의 얼굴피부 및 얕은얼굴지방의 부위별 두께

지도교수 신 동 훈

이 논문을 의학박사 학위논문으로 제출함

2019 년 4 월

서울대학교 대학원

의학과 해부학전공

김 유 수

김유수의 의학박사 학위논문을 인준함

2019 년 7 월

위 원 장 _____ (인)

부위원장 _____ (인)

위 원 _____ (인)

위 원 _____ (인)

위 원 _____ (인)

Regional thickness of the skin and superficial fat in Asian faces

by

You Soo Kim

A thesis submitted to the Department of Anatomy in partial fulfilment of the requirements for the Degree of Doctor of Philosophy in Medicine at Seoul National University College of Medicine

July, 2019

Approved by Thesis committee:

Professor _____Chairman
Professor _____Vice chairman
Professor _____
Professor _____
Professor _____

ABSTRACT

Introduction: The aim of this study was to establish the overall facial skin and superficial fat thicknesses using a 3D scanning system.

Methods: From 53 adult Korean and Thai embalmed adult cadavers, the undissected and serially-dissected facial specimens were scanned and reconstructed. And then, the scanned facial images were superimposed using Morpheus Plastic Solution (version 3.0) software. Finally, the facial skin and superficial fat thicknesses at 75 landmarks on seven facial regions were calculated from the superimposed images.

Results: The facial skin tended to become thicker in the order of the radix and dorsum, and the temple, supraorbital, forehead, perioral, cheek, and infraorbital areas. The skin was thinnest at the radix and dorsum (1.51±0.55 mm), and thickest in the infraorbital region (1.97±0.84 mm). The skin was thinnest at the points on temple (1.25~1.30 mm), and thickest at point where the vertical line passing through the lateral canthus intersects with the transverse line passing through the bilateral alares (2.25±0.77 mm). The facial superficial fat thickness

tended to increase in the order of the radix and dorsum, supraorbital, forehead, temple, cheek, infraorbital, and perioral regions. The superficial fat was thinnest at the radix and dorsum (1.61±1.07 mm), and thickest in the perioral region (5.14±3.31 mm). The superficial fat was thinnest at the rhinion (0.85±0.62 mm) and thickest in the perioral region lateral to the nasolabial fold (8.17±3.02 mm).

Conclusions: The present findings indicate that a 3D scanning system can yield crucial anatomical information about the depths of the facial skin and superficial fat layers for utilization in various minimally invasive clinical procedures.

Keyword : facial skin; superficial facial fat; 3D scanning system; regional thickness

Student Number : 2012-30543

CONTENTS

LIST OF TABLES

LIST OF FIGURES

APPENDIX

LIST OF ABBREVIATIONS

3D scanning : three dimensional scanning

CT : computer tomography

DAO : depressor anguli oris muscle

MDS 3.0 : Morpheus Plastic Solution 3.0

MRI : Magnetic Resonance Image

PDO : polydioxanone

SMAS : superficial musculo-aponeurotic system

T : transverse line

US : ultrasound

V : vertical line

INTRODUCTION

The facial superficial fat is anatomically divided into nasolabial, malar, orbital, forehead, and jowl fat compartments, whose volumes change with age (Lambros 2007; Rohrich and Pessa 2007). Drooping appears in superficial fat due to gravity and relocation, and atrophy takes place due to changes in volume that are not balanced between the superficial and deep fat compartments (Kim et al., 2016). Clinically, the volume of fat contributes to the fullness of a young face, and volumetric changes in fat manifest as aging characteristics of the face, such as nasolabial folds, tear trough deformities, and hollows (Fitzgerald and Rubin 2014; Rohrich et al., 2008).

Various recently introduced minimally invasive treatment modalities such as botulinum toxin and filler injections, and thread lifting are now widely used for enhancing the aging face (Surgeons ASoP. 2017). In a special, filler is used to increase the volume of tissue, and so understanding the regional thickness and distribution of the facial superficial fat is essential for optimizing minimally invasive procedures.

Sagging is also a major aging phenomenon for which surgical corrections have been considered as the only treatment option. However, thread lifting is now widely performed as an alternative procedure for improving facial sagging and relocating facial fat (Gülbitti et al., 2008; Suh et al., 2015). The target layer of the face for thread lifting should be the superficial fat in order to reduce the likelihood of complications and obtain optimal outcomes. For these reasons, it is crucial to understand the regional thickness of the facial superficial fat when performing various minimally invasive procedures.

Several diagnostic imaging devices methodologies such as computed tomography, magnetic resonance imaging, and ultrasonography(US) have been commonly used to investigate the skin and the subcutaneous fat layer (Gülbitti et al., 2008; Schenck et al., 2018; Iyengar et al., 2018; Foissac et al., 2017; Wysong et al., 2014; Gosain et al., 2005). Due to technical limitation such as a localized low imaging resolution, previous studies could not demonstrate the topography of the skin and superficial fat thicknesses over the entire face. 3D scanned images of the face are now widely used for various diagnosis and surgical or nonsurgical evaluations before and after

procedures as well as for facial aesthetics due to the ease of measurements and their high accuracy (Kim et al., 2018; Hammond et al., 2004).

The aim of this study was to establish the overall facial skin and superficial fat thicknesses using a 3D scanning system before and after dissection. Such information about the standard topography of the superficial facial structure in Korean and Thai cadavers can be used in guidelines for minimally invasive procedures.

MATERIALS AND METHODS

Fifty-three embalmed adult Korean and Thai cadavers (35 Koreans and 18 Thais; 32 males and 21 females) aged 52~100 years at death (mean age 76.7 years) and with a mean BMI of 25.9 kg/m^2 (range 18.0~40.4 kg/m^2) were used. None of the cadaveric specimens had congenital malformation, pathological findings, surgery, or trauma. This study was performed in accordance with the principles outlined in the Declaration of Helsinki. Appropriate consents and approval were obtained from the families before using the specimens.

Identification of the facial landmarks

Prior to identifying facial landmarks, we defined 6 vertical and 11 transverse reference lines (Fig.1, Table 1 and 2). Vertical reference lines were defined as both the midline and the lines passing through the pupil, canthus, the medial margins of orbital rim, and the lobule of the auricle.

The transverse reference lines are specified as lines passing through the midpoint between the metopion and the glabellar, the margins of the orbital rim, the cheilion, the mandibular border, and the middle lines of two near transverse reference lines.

82 facial landmarks selected based on the facial region (Fig. 1). The landmarks are: the alare of the nose, zygion, trichion, sellion, rhinion, frontal eminence, and meeting points between vertical reference lines and horizontals reference lines including the point mentioned above.

The face was divided by landmarks into seven regions as the forehead, radix & dorsum, supraorbital, infraorbital, perioral, temple and cheek (Table 3 to 10, Fig. 3c).

3D scanning using a structured-light scanner for the analyses of the facial skin and superficial fat thickness

The facial skin and the superficial fat thicknesses were measured by scanning each specimen in the following three steps using a structured-light 3D scanner (Morpheus3D®, Morpheus Company, Seongnam, Korea): (1) scanning the facial skin surface (first layer of the face), (2) scanning the

superficial fat surface (second layer of the face), and (3) scanning the superficial facial muscle surface (third layer of the face) after removing the superficial fat tissues.

Prior to performing the dissection, the undissected skin surface of face was scanned from its frontal and bilateral oblique aspects (scan 1, Fig. 2A). The obtained 3D scanned images were reconstructed and combined through geometry analysis of the nearby areas at three points (lateral canthus, alare, and cheilion) bilaterally using Morpheus Dental Solution (MDS) software (version 3.0, Morpheus Company, Seongnam, Korea).

After 3D scanning of the facial skin surface, the left half facial skin (deviating slightly right of the midline) was gently dissected and separated from the subcutaneous layer(Fig 3). Careful attention was taken to ensure that the skin was not stretched excessively and to minimize the pressure applied to the subcutaneous layer during the dissection procedure. After separating the skin from the facial superficial fat, each specimen was scanned again using the same process (scan 2, Fig. 2B). For scanning the facial muscle surface, the superficial fat was dissected and then carefully removed from the muscle

and superficial musculo-aponeurotic system (SMAS) surface. After removing the superficial fat, the specimen was scanned again with the 3D scanner from the frontal and bilateral oblique aspects (scan 3, Fig. 2C).

Superimposition of three layers (skin, superficial fat, and muscle layer) using 3D scanned facial images

During the dissection, the right half of the facial skin and the superficial fat were preserved for later use as a reference in the superimposition procedure. Eighty-two landmarks were digitized and aligned on the undissected 3D scanned images (first layer) based on points that had been premarked on the skin surface. After performing digitization, the 3D scanned images of each layer (only two at a time) were superimposed based on the preserved side of the face using MDS 3.0 (Fig. 2D and 2E). Each of the landmarks on the 3D scanned image of the facial skin surface were projected perpendicularly from its tangent onto the 3D scanned image of the dissected image, and the distances between the corresponding points were calculated using MDS 3.0 to automatically determine the facial skin thickness.

Statistical analyses

The statistical calculations and analyses were performed using standard software (SPSS version 23.0 for Windows, SPSS, Chicago, IL, USA). A p value of <.05 was considered statistically significant. Differences in measurement values between males and females were analyzed using Student's t-test. For each age group, the differences in the thicknesses of the skin and the superficial fat averages both of the total and of each region were determined using one-way ANOVA. Depending on age, they were divided into groups of 50 to 69, 70 to 89, and 90 or older.

RESULTS

The thicknesses of the facial skin and the superficial fat in seven regions of the face did not differ significantly for sex and age ($p>.05$), but they did differ between the regions ($p<.01$, Table 12 to 15). The facial skin tended to become thicker in the order of the radix and dorsum, and the temple, supraorbital, forehead, perioral, cheek, and infraorbital areas (Table 10). Among the seven regions, the skin was thinnest at the radix and dorsum (1.51±0.55 mm), and thickest in the infraorbital region (1.97±0.84 mm) (Fig. 4). Across the 75 points measured, the skin was thinnest at the points on temple (#47 and #48) (1.25~1.30 mm), and thickest at point #28 where the vertical line passing through the lateral canthus (V4) intersects with the transverse line passing through the bilateral alares (T7) (2.25±0.77 mm) .

The facial superficial fat thickness tended to increase in the order of the radix and dorsum, supraorbital, forehead, temple, cheek, infraorbital, and perioral regions. The superficial fat was thinnest at the radix and dorsum (1.61±1.07 mm), and thickest in the perioral region (5.14±3.31 mm) (Table 11). The

superficial fat was thinnest at the rhinion (0.85±0.62 mm at point #14) and thickest in the perioral region lateral to the nasolabial fold (8.17±3.02 mm at point #32).

The mean skin thickness in the forehead region was 1.70 mm (Table 10). The thickness of the skin tended to be thicker in the lower than the upper part of the forehead, but the skin tended to be thinner in the lateral than the medial part. The superficial fat did not differ markedly between the upper and the lower part (Table 16, Fig. 4).

The mean skin thickness at both the radix (sellion, #13) and the dorsum (rhinion, #14) was 1.36±0.50mm and 1.42±0.56, respectively. And the corresponding superficial fat thicknesses were 1.61±0.85 mm and 0.85±0.62 mm, respectively ($p<.01$, Table 19).

The skin thickness in the supraorbital region along the transverse line passing through the supraorbital margin (T3) was about 1.67 mm at all measurement points and tended to be thinner in the lateral than the medial part of the supraorbital region (#15 to #18, Table 11), but the superficial fat was thickest at the point on the lateral orbital rim (2.28±1.32 mm at point #18) (Table 17).

There were significant differences in skin thickness in the temple and cheek regions ($p<.05$, Table 9, Fig. 4). The superficial fat in the temple region tended to be slightly thicker from the upper part (mean 2.11 (1.73~2.39) mm at points #40 to #46) to the lower part (mean 2.93(2.54~3.48)mm at points #47 to #54) Table 18).

In the cheek region, the mean superficial fat thickness of the anterior cheek (points #55, #56, #59, #60, #63, #64, #67, #68, #71, and #72) was 4.98 mm (range 3.74~6.30 mm) while the posterior cheek (points #57, #58, #61, #62, #65, #66, #69, #70, #73, and #74) was thinner with a mean of 4.17 mm (range 3.58~4.91mm) (Table 22).

On the zygion (point g), which is at the border between the temple and cheek, the skin and superficial fat thicknesses were 1.68 mm and 3.85 mm, respectively (Tables 11 and 22, Fig. 5).

In the infraorbital and perioral regions, the skin thickness was relatively uniform, ranging from 1.82mm to 1.97 mm ($p>.05$, Table 11), whereas the superficial fat thickness in these regions varied markedly across the measurement points. The superficial fat was thinnest at point #20 in the infraorbital

region (mean of 2.39mm at the level of the inferior orbital rim) and thickest at point #28 in the infraorbital region (mean of 7.84mm in the submalar area) (Table 20, Fig. 5).

The superficial fat in the infraorbital region tended to become thicker (2.39~3.77 mm) from the upper area along the inferior orbital rim (points #19 to #22) to the lower area (5.10~7.84 mm at points 24 to #29), and from the medial area (2.39~6.51 mm) to the lateral area (3.47~7.84 mm) (Table 20). In perioral regions, the skin thickness was relatively uniform, ranging from 1.40 mm to 2.10 mm ($p>.05$, Table 21) whereas the superficial fat thickness in these regions varied markedly across the measurement points. The superficial fat was thinnest at point #34 in the perioral region (1.71 mm at just lateral to the cheilion) and thickest at point #32 in the perioral region (mean of 8.17 mm at lateral to the nasolabial fold) (Table 21, Fig. 5).

Based on the location of the nasolabial fold, the superficial fat was clearly thicker in the lateral perioral region at points #32, #35, and #38 (6.62~8.17 mm) than in the medial perioral region at points #30, #34, and #37 (1.71~3.98 mm) (Table 21, Fig. 5).

Table 1. The Vertical Reference Lines

Lines	Descriptions
V1	Midline passing through the glabella(#12) and rhinion(#13)
V2	Vertical line passing through the medial canthus (a)
V3	Midpupillary line passing through the pupil (b)
V4	Vertical line passing through the lateral canthus (c)
V5	Vertical line passing through the medial margin of the lateral orbital rim (d)
V6	Vertical line passing through the lobule of the auricle

Table 2. The Transverse Reference Lines

Line	Descriptions
T1	Transverse line passing through the midpoint between the metopion(#2) and the glabella(#12)
T2	Transverse line passing through the midpoint between T1 and T3
T3	Transverse line passing through the supraorbital margin
T4	Transverse line passing through the point on the lateral orbital rim (d) at the level of the lateral canthus (c)
T5	Transverse line passing through the inferior orbital rim
T6	Transverse line passing through the midpoint between T5 and T7
T7	Transverse line passing through the nasal alare
T8	Transverse line passing through the midpoint between T7 and T9
T9	Transverse line passing through the bilateral cheilions
T10	Transverse line passing through the midpoint between T9 and T11
T11	Transverse line passing through the mandibular border

Table 3. Anatomical standard facial landmarks

Points	Descriptions
a	Medial canthus
b	Pupil
c	Lateral canthus
d	Lateral orbital rim at the level of lateral canthus (c)
e	Alare of nose
f	Cheilion
g	Zygion
h	Lobule of auricle

Table 4. Anatomical forehead landmarks based on the vertical and transverse reference lines

Points	Descriptions	Region
1	Trichion	forehead
2	Metopion	forehead
3	Half point between Metopion (#2) and Glabella (#12)	forehead
4	Crossing point between V1 and T2	forehead
5	Frontal eminence	forehead
6	Crossing point between V2 and T1	forehead
7	Crossing point between V3 and T1	forehead
8	Crossing point between V4 and T1	forehead
9	Crossing point between V2 and T2	forehead
10	Crossing point between V3 and T2	forehead
11	Crossing point between V4 and T2	forehead
12	Glabella	forehead

Table 6. Anatomical radix & dorsum landmarks based on the vertical and transverse reference lines

Points	Descriptions	Region
13	Sellion	radix & dorsum
14	Rhinion	radix & dorsum

Table 6. Anatomical supraorbital landmarks based on the vertical and transverse reference lines

Points	Descriptions	Region
15	Crossing point between V2 and T3	supraorbital
16	Crossing point between V3 and T3	supraorbital
17	Crossing point between V4 and T3	supraorbital
18	Crossing point between V5 and T3	supraorbital

Table 7. Anatomical infraorbital landmarks based on the vertical and transverse reference lines

Points	Descriptions	Region
19	Crossing point between V2 and T5	infraorbital
20	Crossing point between V3 and T5	infraorbital
21	Crossing point between V4 and T5	infraorbital
22	Crossing point between V5 and T5	infraorbital
23	Crossing point between V2 and T6	infraorbital
24	Crossing point between V3 and T6	infraorbital
25	Crossing point between V4 and T6	infraorbital
26	Crossing point between V5 and T6	infraorbital
27	Crossing point between V3 and T7	infraorbital
28	Crossing point between V4 and T7	infraorbital
29	Crossing point between V5 and T7	infraorbital

Table 8. Anatomical perioral landmarks based on the vertical and transverse reference lines

Points	Descriptions	Region
30	Midpoint of nasolabial fold from alare (e) and cheilion (f)	perioral
31	Crossing point between V3 and T8	perioral
32	Crossing point between V4 and T8	perioral
33	Crossing point between V5 and T8	perioral
34	Crossing point between V3 and T9	perioral
35	Crossing point between V4 and T9	perioral
36	Crossing point between V5 and T9	perioral
37	Crossing point between V3 and T10	perioral
38	Crossing point between V4 and T10	perioral
39	Crossing point between V5 and T10	perioral

Table 9. Anatomical temple landmarks based on the vertical and transverse reference lines

Points	Descriptions	Region
40	Crossing point between V5 and T1	temple
41, 42, 43	1/5, 2/5, and 3/5 points between V5 and V6 at the level of T1	temple
44, 45, 46	1/5, 2/5, and 3/5 points between V5 and V6 at the level of T2	temple
47, 48, 49, 50	1/5, 2/5, 3/5, and 4/5 points between V5 and V6 at the level of T3	temple
51, 52, 53, 54	1/5, 2/5, 3/5, and 4/5 points between V5 and V6 at the level of T4	temple

Table 10. Anatomical cheek landmarks based on the vertical and transverse reference lines

Points	Descriptions	Region
55, 56, 57, 58	1/5, 2/5, 3/5, and 4/5 points between V5 and V6 at the level of T5	cheek
59, 60, 61, 62	1/5, 2/5, 3/5, and 4/5 points between V5 and V6 at the level of T6	cheek
63, 64, 65, 66	1/5, 2/5, 3/5, and 4/5 points between V5 and V6 at the level of T7	cheek
67, 68, 69, 70	1/5, 2/5, 3/5, and 4/5 points between V5 and V6 at the level of T8	cheek
71, 72, 73, 74	1/5, 2/5, 3/5, and 4/5 points between V5 and V6 at the level of T9	cheek

Table 11. Overall mean thicknesses of the facial skin and superficial fat based on the anatomical regions.

Regions	Skin Mean ± SD	Superficial fat Mean ± SD
Forehead	1.70 ± 0.71*	1.99 ± 1.21
Radix & dorsum	1.51 ± 0.55*†	1.61 ± 1.07
Supraorbital	1.67 ± 0.83*	1.82 ± 1.22
Infraorbital	1.97 ± 0.84*†‡	4.93 ± 2.98
Perioral	1.82 ± 0.83†	5.14 ± 3.31
Temple	1.65 ± 0.91*‡	2.58 ± 1.68
Cheek	1.85 ± 1.03†‡	4.54 ± 2.71

Unit : mm, SD: standard deviation

The facial skin thickness

1) *Forehead, radix and dorsum, supraorbital, and temple regions < infraorbital region (P<.01)

2) †Radix and dorsum region < infraorbital, perioral and cheek regions (P<.01)

3) ‡Temple region < infraorbital, cheek regions (P<.01)

The facial superficial fat thickness (P<.01): Radix and dorsum, supraorbital regions, and forehead < perioral and temple regions < infraorbital and cheek regions

Table 12. Overall mean thicknesses of the facial skin between male and female based on the anatomical regions.

Regions	Male Mean ± SD	Female Mean ± SD	P-value
Forehead	1.71 ± 0.81	1.70 ± 0.87	0.903
Radix & dorsum	1.55 ± 0.72	1.49 ± 0.56	0.173
Supraorbital	1.68 ± 0.90	1.66 ± 1.05	0.327
Infraorbital	1.94 ± 0.75	1.98 ± 0.92	0.459
Perioral	1.82 ± 0.83	1.80 ± 0.73	0.885
Temple	1.66 ± 0.87	1.54 ± 0.95	0.382
Cheek	1.82 ± 1.12	1.92 ± 0.92	0.483

Unit : mm, SD: standard deviation

Table 13. Overall mean thicknesses of the superficial fat between men and women based on the anatomical regions.

Regions	Male Mean ± SD	Female Mean ± SD	P-value
Forehead	2.01 ± 1.32	1.98 ± 1.15	0.882
Radix & dorsum	1.63 ± 1.13	1.59 ± 1.24	0.741
Supraorbital	1.85 ± 1.33	1.73 ± 1.22	0.215
Infraorbital	5.03 ± 3.42	4.98 ± 2.65	0.348
Perioral	5.27 ± 3.11	4.55 ± 4.23	0.104
Temple	2.62 ± 1.74	2.54 ± 1.32	0.596
Cheek	4.51 ± 2.81	4.56 ± 2.44	0.543

Unit : mm, SD: standard deviation

Table 14. Overall mean thicknesses of the facial skin depending on age based on the anatomical regions.

Regions	50-69 Mean ± SD	70-89 Mean ± SD	90 or older Mean ± SD	P-value
Forehead	1.61 ± 0.73	2.11 ± 0.88	1.93 ± 0.78	0.687
Radix & dorsum	1.39 ± 0.54	1.46 ± 0.64	1.63 ± 0.68	0.312
Supraorbital	1.39 ± 0.85	1.89 ± 0.98	1.84 ± 1.12	0.326
Infraorbital	1.89 ± 0.84	1.97 ± 079	1.96 ± 0.64	0.541
Perioral	1.72 ± 0.88	1.83 ± 0.92	1.92 ± 0.81	0.422
Temple	1.62 ± 0.83	1.72 ± 0.67	1.66 ± 0.83	0.721
Cheek	1.92 ± 1.15	1.88 ± 1.07	1.83 ± 1.05	0.126

Unit : mm, SD: standard deviation

Table 15. Overall mean thicknesses of the superficial fat depending on age based on the anatomical regions.

Regions	50-69 Mean ± SD	70-89 Mean ± SD	90 or older Mean ± SD	P-value
Forehead	2.07 ± 1.20	1.92 ± 1.38	1.83 ± 1.27	0.157
Radix & dorsum	1.56 ± 0.83	1.62 ± 1.10	1.60 ± 1.05	0.514
Supraorbital	1.99 ± 1.37	1.75 ± 1.13	1.81 ± 1.55	0.641
Infraorbital	5.12 ± 3.10	5.20 ± 3.50	5.26 ± 2.95	0.815
Perioral	5.16 ± 3.27	6.01 ± 2.90	4.17 ± 2.22	0.101
Temple	2.86 ± 2.00	2.42 ± 1.11	2.31 ± 1.89	0.352
Cheek	4.49 ± 2.66	4.22 ± 2.18	4.34 ± 2.39	0.462

Unit : mm, SD: standard deviation

Table 16. Mean thicknesses of the facial skin and superficial fat on 11 anatomical forehead landmarks

Regions	Points	Skin Mean ± SD	Superficial fat Mean ± SD
Forehead	1	1.49 ± 0.77	1.55 ± 0.98
	2	1.58 ± 0.59	1.74 ± 1.05
	3	1.62 ± 0.61	1.95 ± 1.20
	4	1.57 ± 0.61	2.28 ± 1.25
	5	1.74 ± 0.68	1.71 ± 1.00
	6	1.77 ± 0.73	2.28 ± 1.25
	7	1.61 ± 0.63	2.12 ± 1.19
	8	1.54 ± 0.78	2.07 ± 1.39
	9	2.07 ± 0.67	1.89 ± 1.11
	10	2.05 ± 0.71	2.04 ± 1.22
	11	1.69 ± 0.78	2.21 ± 1.43

Unit : mm, SD: standard deviation

Table 17. Mean thicknesses of the facial skin and superficial fat on 4 anatomical Supraorbital landmarks

Regions	Points	Skin Mean ± SD	Superficial fat Mean ± SD
Supraorbital	15	1.83 ± 0.72	2.02 ± 1.30
	16	1.65 ± 0.80	1.59 ± 0.89
	17	1.61 ± 0.85	1.44 ± 1.19
	18	1.58 ± 0.98	2.28 ± 1.32

Unit : mm, SD: standard deviation

Table 18. Mean thicknesses of the facial skin and superficial fat on 15 anatomical Temple landmarks

Regions	Points	Skin Mean ± SD	Superficial fat Mean ± SD
Temple	40	1.64 ± 0.95	2.12 ± 1.04
	41	1.71 ± 0.91	1.96 ± 1.11
	42	1.69 ± 0.80	2.20 ± 1.36
	43	1.65 ± 0.87	1.73 ± 1.25
	44	1.33 ± 0.85	2.07 ± 1.47
	45	1.54 ± 0.80	2.34 ± 1.53
	46	1.95 ± 1.08	2.39 ± 1.23
	47	1.30 ± 1.01	2.54 ± 1.58
	48	1.25 ± 0.74	2.73 ± 1.68
	49	1.69 ± 0.96	2.83 ± 1.73
	50	1.86 ± 0.85	2.63 ± 1.85
	51	1.58 ± 0.88	2.73 ± 1.68
	52	1.53 ± 0.85	3.48 ± 2.07
	53	1.84 ± 0.93	3.44 ± 1.88
	54	1.86 ± 1.03	3.06 ± 2.24

Unit : mm, SD: standard deviation

Table 19. Mean thicknesses of the facial skin and superficial fat on 3 anatomical Dosum and Radix landmarks

Regions	Points	Skin Mean ± SD	Superficial fat Mean ± SD
Dorsum and radix	12	1.76 ± 0.53	2.23 ± 1.17
	13	1.36 ± 0.50	1.61 ± 0.85
	14	1.42 ± 0.56	0.85 ± 0.62

Unit : mm, SD: standard deviation

Table 20. Mean thicknesses of the facial skin and superficial fat on 11 anatomical Infraorbital landmarks

Regions	Points	Skin Mean ± SD	Superficial fat Mean ± SD
Infraoribtal	19	1.67 ± 0.77	2.97 ± 1.72
	20	1.54 ± 0.61	2.39 ± 1.79
	21	1.93 ± 0.79	3.47 ± 2.04
	22	2.03 ± 0.93	3.77 ± 2.01
	23	1.53 ± 0.77	2.67 ± 2.03
	24	2.18 ± 0.71	5.10 ± 2.35
	25	2.02 ± 0.86	5.52 ± 2.42
	26	2.02 ± 0.89	5.38 ± 2.65
	27	2.14 ± 0.90	6.51 ± 2.61
	28	2.25 ± 0.77	7.84 ± 2.82
	29	2.23 ± 0.85	7.22 ± 3.38

Unit : mm, SD: standard deviation

Table 21. Mean thicknesses of the facial skin and superficial fat on 10 anatomical Perioral landmarks

Regions	Points	Skin Mean ± SD	Superficial fat Mean ± SD
Perioral	30	1.90 ± 0.77	3.19 ± 1.96
	31	2.00 ± 0.75	3.70 ± 2.41
	32	1.97 ± 0.88	8.17 ± 3.02
	33	2.10 ± 0.83	7.36 ± 3.22
	34	1.40 ± 0.68	1.71 ± 1.04
	35	1.81 ± 0.79	6.62 ± 2.71
	36	1.59 ± 1.10	2.16 ± 1.17
	37	1.83 ± 0.76	3.98 ± 1.78
	38	1.64 ± 0.72	6.71 ± 3.03
	39	1.82 ± 0.86	6.45 ± 3.31

Unit : mm, SD: standard deviation

Table 22. Mean thicknesses of the facial skin and superficial fat on 20 anatomical Cheek landmarks

Regions	Points	Skin Mean ± SD	Superficial fat Mean ± SD
Cheek	g (zygion)	1.68 ± 0.92	3.81 ± 2.13
	55	1.83 ± 1.14	3.96 ± 2.28
	56	1.72 ± 0.83	4.22 ± 2.40
	57	1.80 ± 1.21	3.93 ± 2.10
	58	1.89 ± 1.09	3.60 ± 2.71
	59	1.86 ± 1.05	5.19 ± 2.73
	60	1.68 ± 0.84	5.07 ± 2.56
	61	1.70 ± 1.06	3.92 ± 2.27
	62	2.05 ± 1.12	3.52 ± 2.47
	63	1.79 ± 0.94	6.36 ± 2.90
	64	1.74 ± 0.80	4.54 ± 2.57
	65	1.75 ± 0.90	4.22 ± 2.18
	66	2.21 ± 1.29	3.86 ± 2.30
	67	2.05 ± 0.86	5.20 ± 2.72
	68	1.70 ± 0.83	4.28 ± 2.39

Table 22. (continued) Mean thicknesses of the facial skin and superficial fat on 20 anatomical Cheek landmarks

Regions	Points	Skin Mean ± SD	Superficial fat Mean ± SD
Cheek	69	1.80 ± 0.90	4.74 ± 2.92
	70	2.14 ± 1.23	4.16 ± 2.66
	71	2.00 ± 1.02	5.49 ± 3.12
	72	1.63 ± 0.93	5.10 ± 3.27
	73	1.97 ± 1.24	4.99 ± 2.97
	74	2.14 ± 1.43	3.87 ± 2.53

Unit : mm, SD: standard deviation

V1
T11
V3
V4
V5
T10
T9
T8
T7
T6
T5
T4
T3
T2
T1
V2
V5
T11
V6
T9
T8
T7
T6
T5
T4
T3
T2
T1

Figure 1. Anatomical facial landmarks for measuring the facial skin and superficial fat thickness. See table 1 for the detailed descriptions of each reference line and landmark.


A
B
C
D
E
F

Figure 2. Reconstruction of 3D scanned images of a cadaveric face using MDS 3.0. The undissected face scanning images (scan 1) were acquired at the frontal and bilateral oblique aspects (A). After separating the skin from the facial superficial fat, the specimen was scanned again with same process (scan 2) (B). For the scanning of facial muscle surface, the superficial fat was dissected and carefully removed from the muscle and superficial musculo-aponeurotic system (SMAS) surface. After removing the superficial fat, the specimen was scanned again with 3D scanner from the frontal and bilateral oblique aspects (scan 3) (C). Superimposition of 3D reconstructed images from two different layers of faces between scan 1 and 2 (D), and between scan 2 and 3 (E) using MPS 3.0. The green colored areas (D and E) indicate the depth difference between two layers. The procedure of the scanning (F).

Figure 3. A photograph showing the skin dissection procedure to reveal the superficial facial fat

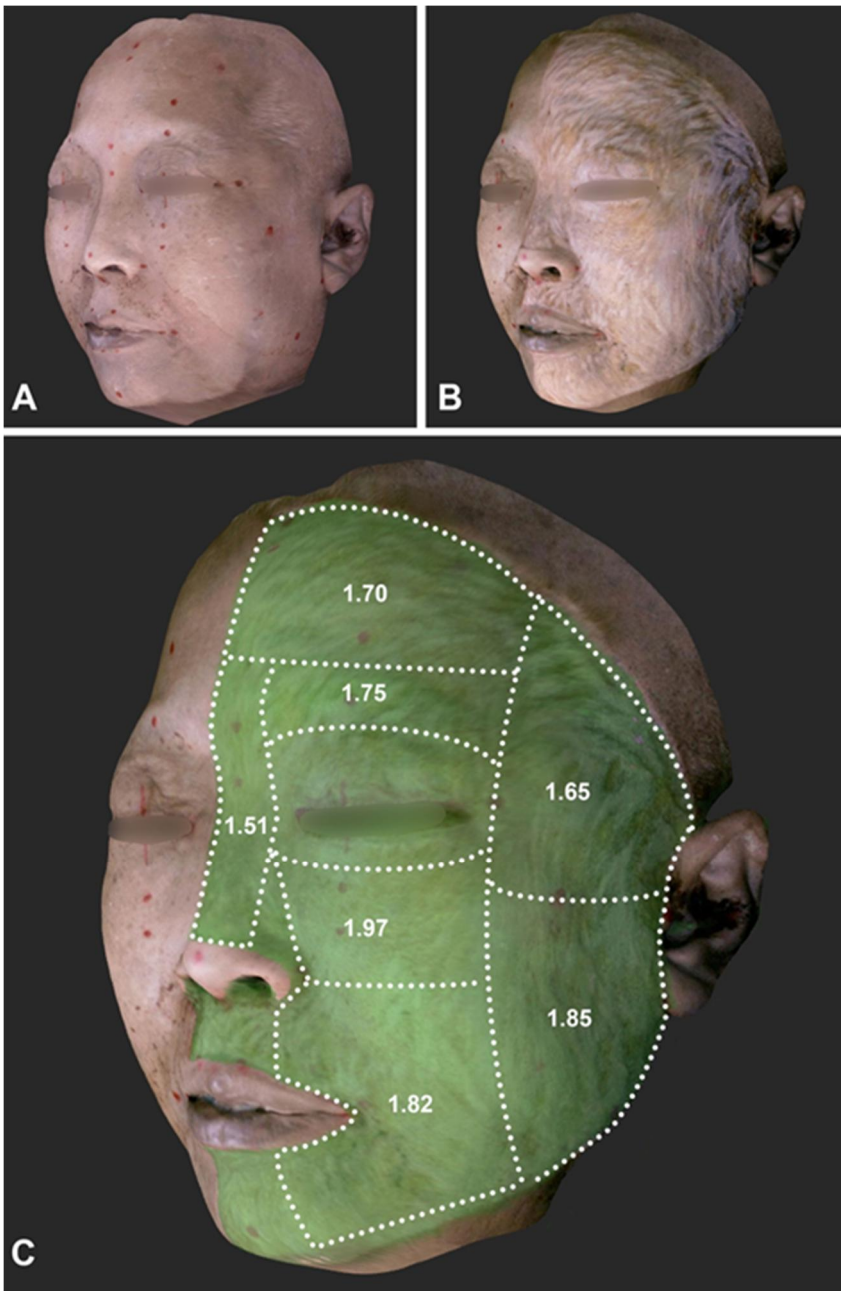

Figure 4. Superimposed 3D image reconstructed from two different layers of the faces. Undissected (scan 1, A) and dissected 3D scanned image after

removal of the facial skin (scan 2, B) were superimposed using MDS 3.0

Figure 4. continued

program (C). Based on the anatomical regions of the face, the mean value of skin thickness is shown (mm). See the details of the skin thick ness in Table 2 and 3.

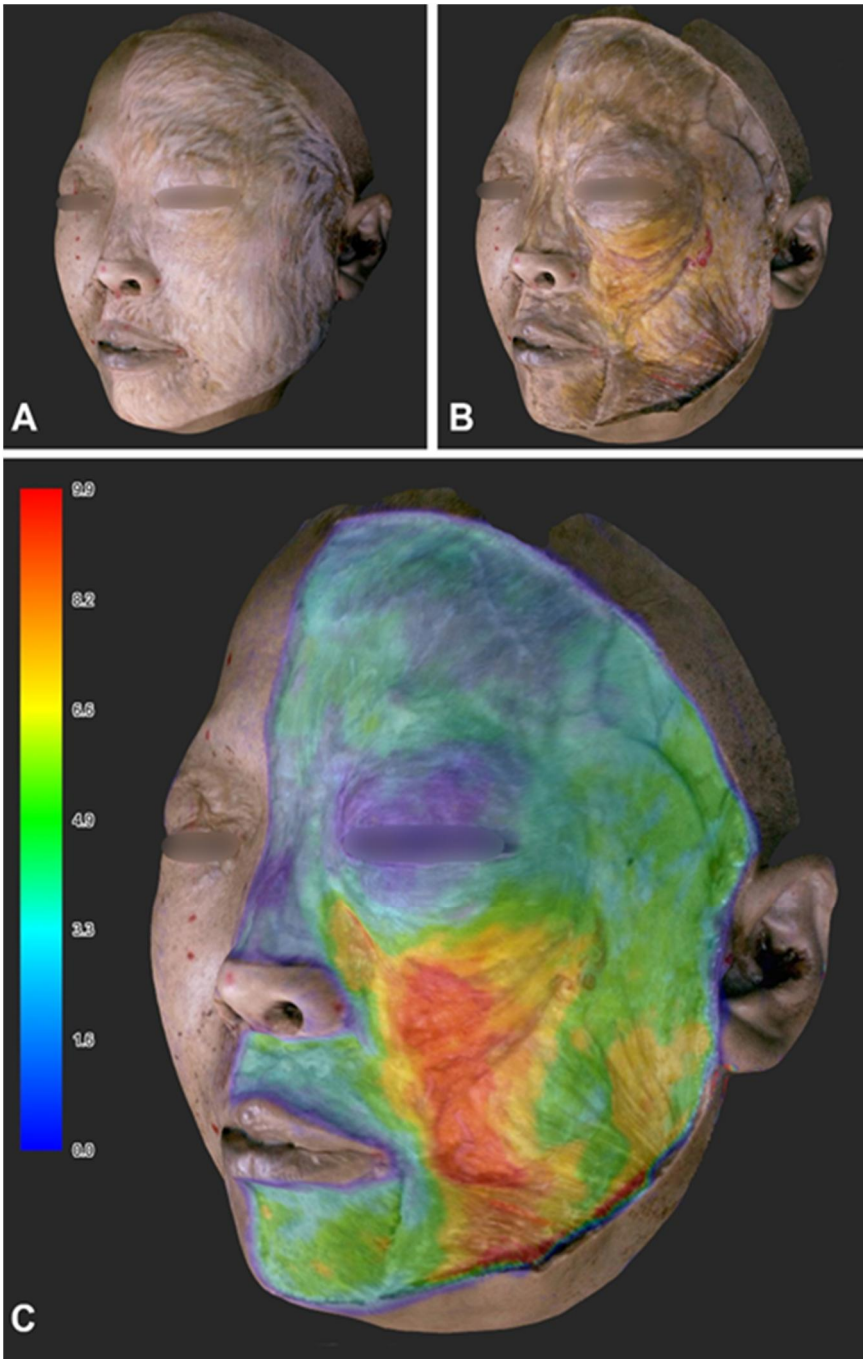
A
B
C

Figure 5. Superimposed 3D image reconstructed from two different layers of the faces. Dissected 3D scanned images after removal of the facial skin (scan 2, A) and the facial superficial fat (scan 3, B) were superimposed using MDS 3.0 program (C). A color bar indicates the thickness of the facial superficial fat (mm).

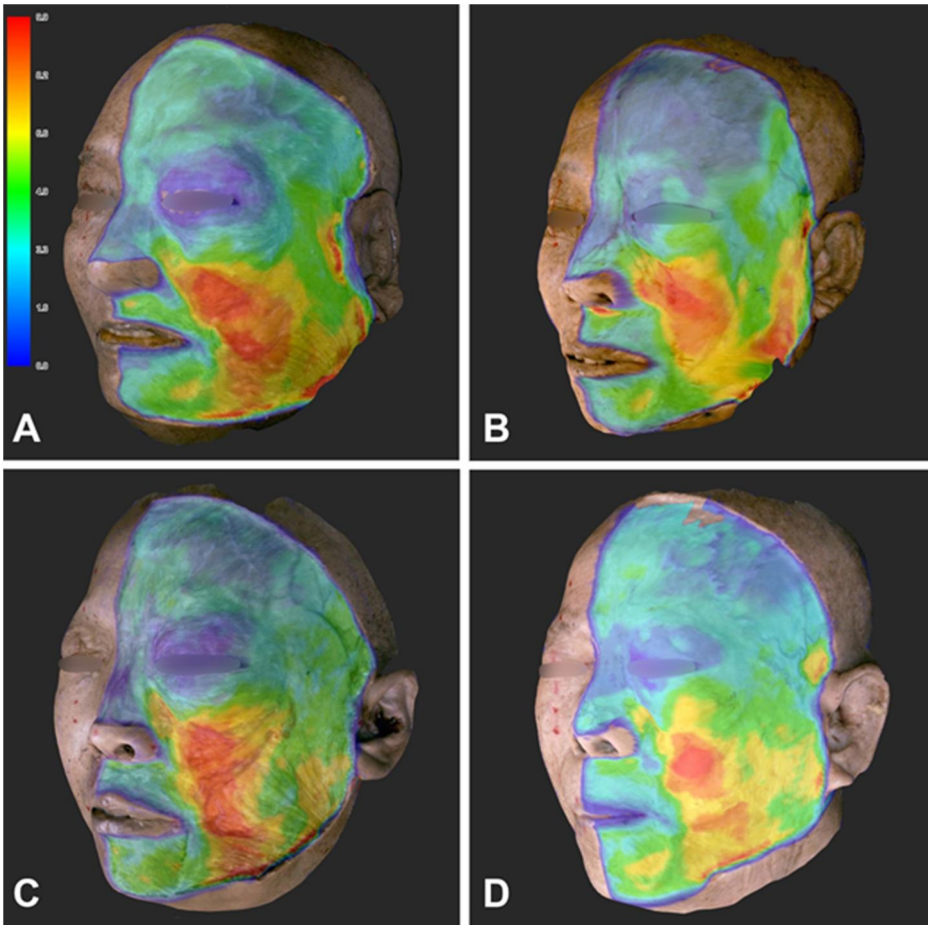

Figure 6. Superimposed 3D images demonstrating the various regional thickness of the facial superficial fat (A~D) using MDS 3.0 program (C). A color bar indicates the differences of the facial superficial fat thickness (mm).

DISCUSSION

Recent trends in cosmetic surgery have shifted from surgery to minimally invasive procedures such as botulinum toxin and filler injections, and thread lifting. The American Society of Plastic Surgeons reported that the number of cosmetic surgical procedures reduced by approximately 6% over the past 2 decades (from 1.9 million in 2000 to 1.79 million in 2017), while cosmetic minimally invasive procedures such as treatments involving injectables increased by 186% over the same period (from 5.5 million to 15.71 million), of which 7.2 million involved botulinum toxin and 2.7 million involved fillers (Surgeons ASoP. 2017).

Both the 3D injection depth and the 2D injection points have been emphasized in minimally invasive procedures involving botulinum toxin and filler injections, and thread lifting. The target layers in treatments involving injectables can be the facial skin, superficial fat, and muscle layers.

In-depth morphological studies of the human body have been performed using various diagnostic imaging devices. Previous studies that have employed MRI have encountered

difficulties in providing in-depth data for the main anatomical structures of the face because of poor image resolution due to spatial limitations of the head coil (Schenck et al., 2018). The histology method is limited by soft tissue deformation during tissue processing (Chopra et al., 2015). It is now possible for the obtained data to be displayed as 3D images to facilitate the presentation of locational information for utilization in both research and clinical applications. Lee et al. reported that the skin thicknesses obtained objectively using a 3D scanning system before and after facial skin dissection were in good agreement with measurements made using US (Lee et al., 2017).

In our previous study we demonstrated the validity and reliability of measurements with the Morpheus3D® system (Lee et al., 2017). This 3D scanning system is based on structured light and acquires distance information using active triangulation technique, which is advantageous because it captures precise data in a single image. A white light-emitting diode was used as light source in the scanning imaging unit, with the manufacturer claiming a spatial accuracy of better than 0.1mm. Though the measurement differences between living persons and cadavers

could be existed, since the measurement discrepancy is generally uniformly observed and the difference is known to be insignificant. It is reasonable in applying the data from the cadaveric specimens to the actual clinical application.

The targets in most botulinum toxin injection procedures are muscles, while dermal injection techniques involving compounds such as mesotoxin and dermotoxin targeting the skin layer have been spotlighted in many Asian countries, including Korea (Lee et al., 2017; Wu 2015). When a dermal effect such as sebum inhibition is targeted, the active substance is usually injected within skin layer, and so the facial skin thickness should be considered prior to performing the injection.

General data on the facial skin thickness has been obtained from biopsies and US imaging systems as well as 3D scanning (Chopra et al., 2015; Lee et al., 2017; Hwang et al., 2006). Knowledge of the skin and superficial fat thicknesses will allow the approximate injection depth for a target muscle to be determined. Until now there were no depth guidelines for botulinum toxin injection procedures considering the depth of facial muscles, with instead only vague guidelines such as

descriptions of “deep” or “shallow” injections having been documented in most publications.

The present study demonstrated that the facial skin became thicker going toward the lower aspect of the face (means of 1.82 to 1.97 mm) (Table 9). These data are also useful for determining the cannula entry point when injecting filler. It is generally preferable to puncture an area of thicker skin and superficial fat when inserting a cannula, because this can avoid skin problems such as skin damages, bruising, lumps, and other irregularities and can help smooth proceeding of the cannula. The present study found that the skin was thicker at points #28 (2.25±0.77mm) and #29 (2.23±0.85mm). These points are the conventionally used cannula entry points in various filler injection procedures. In particular, point #28—where V4 intersects with T7—is a well-known target cannula puncture point for treating the nasojugal groove or tear trough, and is characterized by a thick layer of underlying superficial fat (7.84±2.82 mm). This explains why a point on the face with both thick skin and thick superficial fat is anatomically highly favorable for performing filler injection procedures (Tables 11 to 22). Compared to the histology method, the skin thickness in

this study was slightly greater than the data by Chopra et al. (2015).

However, anatomical features besides the skin thickness should also be considered during botulinum toxin injection procedures. The upper lip elevators, mouth constrictor, and dilators are concentrated in perioral and infraorbital regions including the cheek, and are covered by 1.88–1.97 mm of facial skin. When performing dermal botulinum toxin treatments in these regions, a meticulous superficial injection that considers the skin thickness is recommended for avoiding the occurrence of facial asymmetry due to the botulinum toxin diffusion into the neighboring facial muscles.

While the facial skin thickness did not differ markedly in the same region, there were distinct differences in the facial superficial fat thickness between points within the same region. The superficial fat in the lower forehead region (points #9 to #11) became thicker from the medial to the lateral part. When injecting filler using a blunt cannula, an entry point on the lateral forehead may be advantageous for inserting, cannulating, and progressing the cannula (Table 11).

In the temple region, the superficial facial fat tended to become thicker from the upper to the lower part, and was slightly thinner in the anterior than the posterior temple region. These results indicate trends similar to previous findings, and was slightly thinner in the anterior than the posterior temple region (Foissac et al., 2017). It is thought to be due to the lack of volume in the upper anterior area in most aged persons. On the other hand, the superficial fat was thicker in the anterior cheek region (mean of 4.98 mm and range 3.74~6.30 mm) than in the posterior cheek region (mean of 4.17 mm and range 3.58~4.91 mm) in the present study (Table 18, 22).

Even though the target of filler injection for soft tissue augmentation is the superficial fat layer, the injection depth and layer have been modified according to the treatment area due to the occurrence vascular accidents such as skin necrosis, blindness, and stroke resulting from intravascular injections (Kim etl al., 2016; Fitzgerald and Rubin 2014; Rohrich et al., 2008). Performing shallow filler injections into the dermis for enhancing the glabella frown line and nasolabial crease injection is relatively safe. Since the measured skin thicknesses at the glabella (point #12) and the nasolabial fold (point #30) were

1.76±0.53 mm and 1.90±0.77 mm, respectively, caution should be taken to inject any deeper than this at these points (Table 16, 21, Fig. 3).

The superficial fat volume of the infraorbital and perioral regions was significantly greater at the lower than the upper area, which confirms the trends found in previous studies (Schenck et al., 2018; Wysong et al., 2014; Gierloff et al., 2012). Based on these results, it is better to consider this area for volume restoration using filler, since the superficial fat volume of the upper area of the infraorbital region can naturally reduce with age. The perioral region also showed a difference in the superficial facial fat thickness, with the lateral perioral area (lateral to the nasolabial fold) being thicker than the medial perioral region (medial to the nasolabial fold). The nasolabial fold can become deeper and longer with age due to sagging of the skin and the malar fat pad, atrophy of the deep medial cheek fat, and changes in the fat composition (Kim et al., 2016). Such aging of the nasolabial fold was similarly observed in the present study, and so fillers should be injected into the medial hollow areas while allowing for the contour of the fat layer (Table 17, 21, Fig. 4).

In the thread-lifting procedure, threads (and especially absorbable types) should be placed in the superficial fat layer above the SMAS and facial muscles to ensure safe and effective outcome (Kim et al., 2016; Suh et al., 2015). If the threads are placed too superficially, skin dimpling or perforation can occur, and perioral muscles may get caught by the inserted threads, resulting in inconvenience during mouth movements when the threads are inserted deep to the SMAS. Moreover, there is a possibility of direct or traction injury to facial nerves and arteries because the nerve and arterial branches generally travel under the SMAS (Kim et al., 2017).

Threads for vertical lifting are usually inserted in the temple region. Using an insertion point near the lower posterior area of the temple where the superficial fat is relatively thick may help to prevent extrusion of the thread end. In particular, the location of the facial nerve and the thickness of the superficial fat should both be considered when determining the passage of the thread over the zygomatic arch. It is known that the temporal branches of the facial nerve closely about the periosteum of the zygomatic arch (Trussler et al., 2010).

Based on our anatomical finding for the thickness of superficial fat at the zygion (point g), the threads should be placed within the subcutaneous tissue layer at a depth of about 5.5 mm from the skin surface in order to prevent injury to the facial nerve branches during the thread insertion procedure (Table 22, Fig. 4).

On the other hand, the superficial fat became thicker at points #35, #38, and #39 due to the formation of a jowl with age. This area is the natural target of fat-resolving injections and for volume redisposition through the thread-lifting procedure by the placing of the thread ends. In addition, caution is necessary to ensure that the threads are inserted at a constant depth from the posterior to the anterior cheek, since the superficial fat volume of the anterior cheek is greater than that of the posterior cheek (Table 22, Figure 4).

In the thread-lifting procedure, threads (and especially absorbable types) should be placed in the superficial fat layer above the SMAS and facial muscles to ensure safe and effective outcome (Suh et al., 2015; Kim et al., 2017). If the threads are placed too superficially, skin dimpling or perforation can occur, and perioral muscles may get caught by the inserted threads,

resulting in inconvenience during mouth movements when the threads are inserted deep to the SMAS. Moreover, there is a possibility of direct or traction injury to facial nerves and arteries because the nerve and arterial branches generally travel under the SMAS (Kim et al. 2017).

Threads for vertical lifting are usually inserted in the temple region. Using an insertion point near the lower posterior area of the temple where the superficial fat is relatively thick may help to prevent extrusion of the thread end. In particular, the location of the facial nerve and the thickness of the superficial fat should both be considered when determining the passage of the thread over the zygomatic arch. It is known that the temporal branches of the facial nerve closely about the periosteum of the zygomatic arch (Trussler et al. 2010). Based on our anatomical finding for the thickness of superficial fat at the zygion (point g), the threads should be placed within the subcutaneous tissue layer at a depth of 3.5 mm in order to prevent injury to the facial nerve branches during the thread insertion procedure (Table 11, Figure. 4 and 5).

The facial skin was thinnest at point #34 in the perioral region. It is recommended to not position the end of threads

around the mouth corner in order to avoid the risk of them protruding. On the other hand, the superficial fat became thicker at points #35, #38, and #39 due to the formation of a jowl with age. This area is the natural target of fat-resolving injections and for volume redisposition through the thread-lifting procedure by the placing of the thread ends. In addition, caution is necessary to ensure that the threads are inserted at a constant depth from the posterior to the anterior cheek, since the superficial fat volume of the anterior cheek is greater than that of the posterior cheek (Table 11, Figs. 4 and 5).

The present study demonstrated 3D scanning and serial facial dissections to produce in-depth anatomical data that has previously been impossible to obtain. Since treatments involving injectables are performed blindly, it is essential to understand the detailed regional topography and thickness of the superficial facial soft tissues to ensure the accuracy and safety of these clinical procedures. Therefore, an in-depth morphological study using 3D scanning can yield depth data on the main blood vessels, muscles, and nerves of the facial area that were previously impossible to obtain. Furthermore, this

provides crucial anatomical knowledge that can be utilized in various minimally invasive clinical procedures.

BIBLIOGRAPHY

Chopra K, Calva D, Sosin M, Tadisina KK, Banda A, De La Cruz C, et al. A Comprehensive Examination of Topographic Thickness of Skin in the Human Face. Aesthetic Surgery Journal. 2015;35(8):1007-13.

Fitzgerald R, Rubin AG. Filler placement and the fat compartments. Dermatologic clinics. 2014;32(1):37-50.

Foissac R, Camuzard O, Piereschi S, Staccini P, Andreani O, Georgiou C, et al. High-Resolution Magnetic Resonance Imaging of Aging Upper Face Fat Compartments. Plast Reconstr Surg. 2017;139(4):829-37.

Gierloff M, Stöhring C, Buder T, Gassling V, Açil Y, Wiltfang J. Aging changes of the midfacial fat compartments: a computed tomographic study. Plastic and reconstructive surgery. 2012;129(1):263-73.

Gosain AK, Klein MH, Sudhakar PV, Prost RW. A volumetric analysis of soft-tissue changes in the aging midface using high-resolution MRI: implications for facial rejuvenation. Plastic and reconstructive surgery. 2005;115(4):1143-52.

Gülbitti HA, Colebunders B, Pirayesh A, Bertossi D, van der Lei B. Thread-Lift Sutures: Still in the Lift? A Systematic Review of the Literature. Plastic and reconstructive surgery. 2018;141(3):341e-7e.

Hammond P, Hutton TJ, Allanson JE, Campbell LE, Hennekam RC, Holden S, et al. 3D analysis of facial morphology. American journal of medical genetics Part A. 2004;126(4):339-48.

Hwang K, Kim DJ, Hwang SH. Thickness of Korean upper eyelid skin at different levels. J Craniofac Surg. 2006;17(1):54-6.

Iyengar S, Makin IR, Sadhwani D, Moon E, Yanes AF, Geisler A, et al. Utility of a High-Resolution Superficial Diagnostic Ultrasound System for Assessing Skin Thickness: A Cross-Sectional Study. Dermatologic Surgery. 2018;44(6):855-64.

Kim B, Oh S, Jung W. The art and science of thread lifting with pinch anatomy. Republic of Korea: Medbook; 2017. 376 p.

Kim H-J, Seo KK, Lee H-K, Kim J. Clinical Anatomy of the Face for Filler and Botulinum Toxin Injection. 1st ed: Singapore, Springer Verlag; 2016.

Kim S-C, Kim HB, Jeong WS, Koh KS, Huh CH, Kim HJ, et al.

Comparison of Facial Proportions Between Beauty Pageant Contestants and Ordinary Young Women of Korean Ethnicity: A Three-Dimensional Photogrammetric Analysis. Aesthetic plastic surgery. 2018;42(3):748-58.

Lambros V. Observations on periorbital and midface aging. Plast Reconstr Surg. 2007;120(5):1367-76; discussion 77.

Lee KW, Kim SH, Gil YC, Hu KS, Kim HJ. Validity and reliability of a structured-light 3D scanner and an ultrasound imaging system for measurements of facial skin thickness. Clinical Anatomy. 2017;30(7):878-86.

Rohrich RJ, Pessa JE, Ristow B. The youthful cheek and the deep medial fat compartment. Plastic and reconstructive surgery. 2008;121(6):2107-12.

Rohrich RJ, Pessa JE. The fat compartments of the face: anatomy and clinical implications for cosmetic surgery. Plastic and reconstructive surgery. 2007;119(7):2219-27.

Schenck TL, Koban KC, Schlattau A, Frank K, Sykes JM, Targosinski S, et al. The Functional Anatomy of the Superficial Fat Compartments of the Face: A Detailed Imaging Study. 2018;141(6):1351-9.

Suh DH, Jang HW, Lee SJ, Lee WS, Ryu HJ. Outcomes of

polydioxanone knotless thread lifting for facial rejuvenation. Dermatol Surg. 2015;41(6):720-5.

Surgeons ASoP. 2017 Plastic Surgery Statistics Report: American Society of Plastic Surgeons; 2018 [Available from: https://www.plasticsurgery.org/documents/News/Statistics/2017/plastic-surgery-statistics-report-2017.pdf.

Trussler AP, Stephan P, Hatef D, Schaverien M, Meade R, Barton FE. The frontal branch of the facial nerve across the zygomatic arch: anatomical relevance of the high-SMAS technique. Plast Reconstr Surg. 2010;125(4):1221-9.

Wu WT. Microbotox of the Lower Face and Neck: Evolution of a Personal Technique and Its Clinical Effects. Plast Reconstr Surg. 2015;136(5 Suppl):92s-100s.

Wysong A, Kim D, Joseph T, MacFarlane DF, Tang JY, Gladstone HB. Quantifying soft tissue loss in the aging male face using magnetic resonance imaging. Dermatologic Surgery. 2014;40(7):786-93.

Appendix

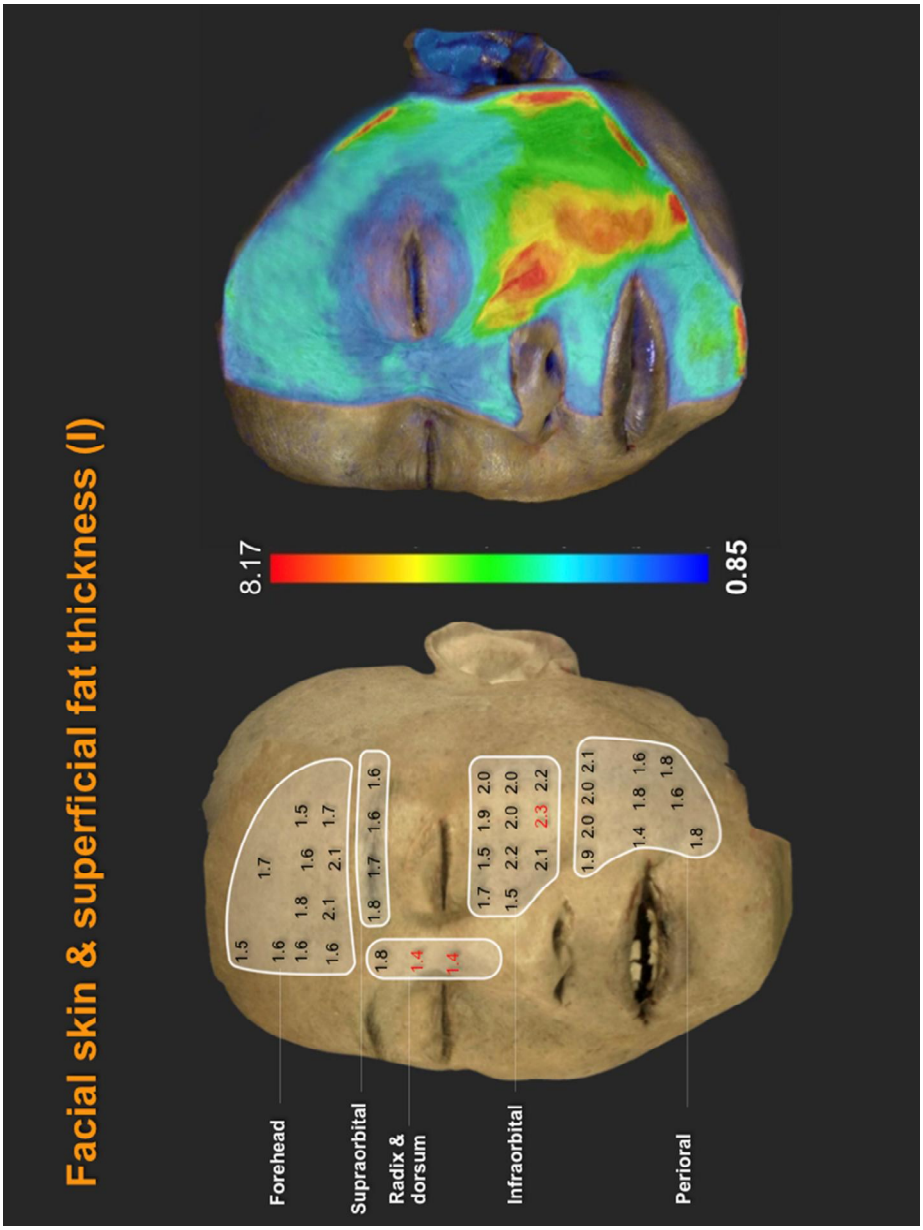

Appendix 1. Average thickness of the facial skin and superficial fat thickness (frontal aspect)

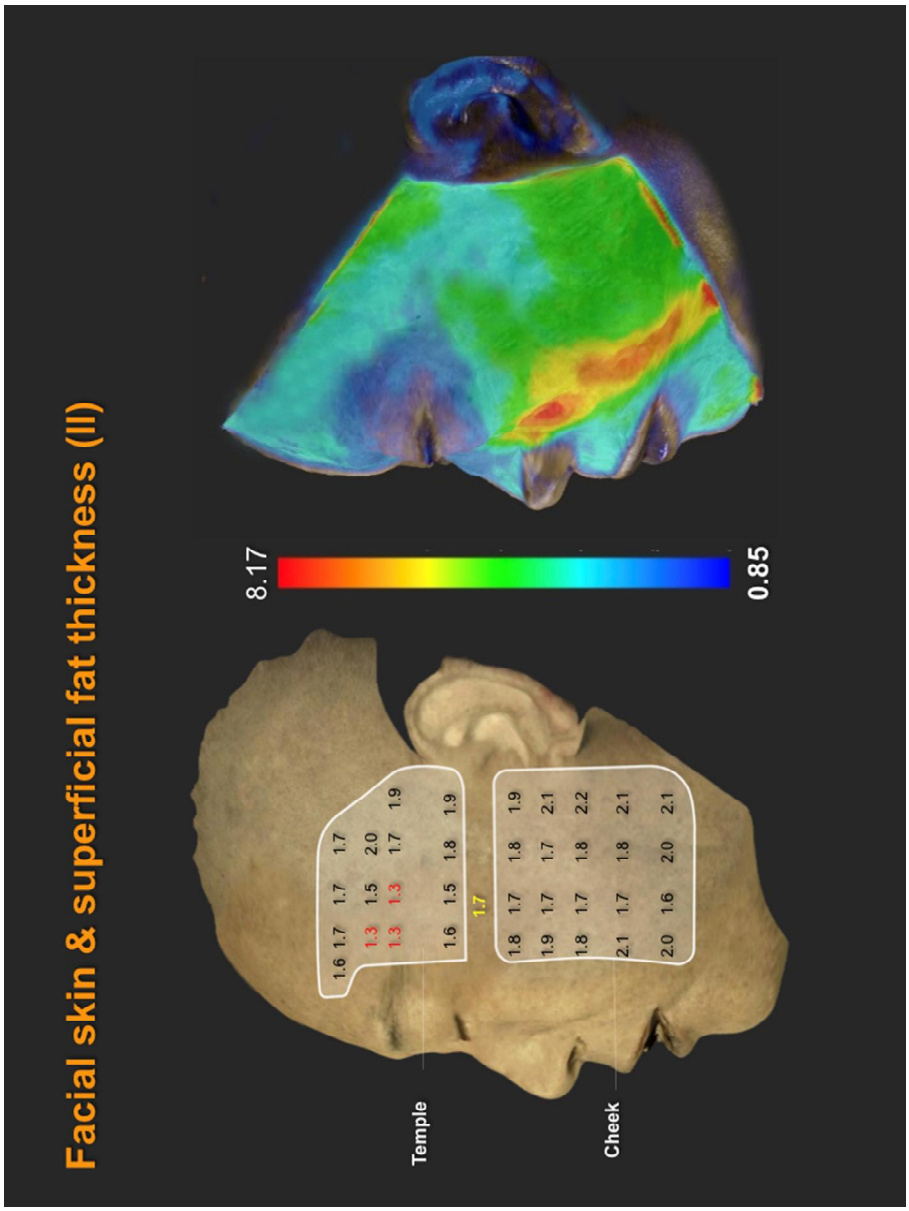

Appendix 2. Average thickness of the facial skin and superficial fat thickness (lateral aspect)

국문초록

서론: 이 연구의 목적은 3D 스캐닝 시스템을 사용하여 전체 얼굴 피부와 얕은지방층의 두께를 확립 하는 것이다.

방법: 53 명의 성인 한국인과 태국인의 고정된 성인 시체에서, 얼굴을 층별로 해부한 후 스캔하여 재구성하였다. 그리고 스캔한 얼굴 이미지들을 Morpheus Plastic Solution (버전 3.0) 소프트웨어를 사용하여 서로 중첩 시켰다. 최종적으로, 7 개의 얼굴 영역, 75 개의 표지점에서의 얼굴 피부 및 표면 지방 두께가 중첩된 이미지로부터 계산되었다.

결과: 얼굴 피부는 코뿌리와와 콧등, 관자, 눈확위, 눈확아래, 이마, 입주위, 뺨과 눈확아래 부위 순으로 두꺼워졌다. 피부는 코뿌리와 콧등 (1.51 ± 0.55 mm)에서 가장 얇고, 눈확아래 부위에서는 가장 두꺼웠다 (1.97 ± 0.84 mm). 피부는 관자부위(1.25 ~ 1.30 mm)의 한점에서 가장 얇고 동공중간선이 양측 콧방울 (2.25 ± 0.77 mm)을 통과하는 가로선과 교차하는 지점에서 가장 두꺼웠다. 얼굴의 얕은지방층 두께는 코뿌리와 콧등, 눈확위, 이마, 관자, 뺨, 아래눈확과 입주위 부위의 순서로 증가하는 경향이 있었다. 얕은지방층은 코뿌리와 콧등 (1.61 ± 1.07 mm)에서 가장 얇았으며, 입주위(5.14 ± 3.31 mm)에서 가장 두꺼웠다. 얕은지방층은 코뼈점 (0.85 ± 0.62 mm)에서 가장 얇았고 코입술주름(8.17 ± 3.02 mm)의 가쪽 연접 영역에서 가장 두꺼웠다.

결론: 본 연구 결과는 3D 스캐닝 시스템이 다양한 최소 침습적 임상 절차에서 활용하기 위해 얼굴 피부 및 얕은지방층의 깊이에 대한 중요한 해부학 적 정보를 산출할 수 있음을 나타낸다.

키워드 : 얼굴피부, 얕은피부지방, 3D 스캐닝시스템, 국소 두께

학번 : 2012-30543

감사의 글

박사과정을 수료한 후 많은 시간이 흘렀고 그 사이에 개인적으로는 정말 많은 변화가 있었습니다. 대치동에서의 개업과 폐업, 벤처사업, 출판, 방송, 정부과제, 해외 법인 설립까지. 이제 정규 교육의 마지막 단계인 박사학위를 받는 시간이 왔습니다. 여태까지 정말 많은 일을 하면서 오늘 날의 제가 만들어졌고 감사해야 할 분이 너무 많습니다.

지도교수님인 신동훈 교수님은 저를 학위과정에 받아주셨을 뿐 아니라 논문이 완성될 때까지 묵묵히 기다려주시고 지지해주셨습니다. 그리고 심사를 해주시고 좋은 논문이 될 수 있도록 조언을 아끼지 않으신 조비룡 교수님을 비롯 강재승, 김명주, 임재영 교수님께도 감사의 말씀을 드립니다. 무엇보다 이 논문은 김희진 교수님의 도움이 없었다면 세상에 나오지 못했을 것입니다. 김 교수님은 논문 뿐 아니라 많은 면에서 모범을 보이시고 저희 형제를 물심양면으로 도와주신 은인이십니다. 같이 고생한 이강우 선생께도 감사합니다.

무엇보다 이 논문이 나오기를 가장 기다리고 계셨던 부모님께도 감사의 말씀을 빼놓을 수가 없습니다. 부모님의 헌신적인 지원과 지지로 박사학위를 받을 수 있었습니다. 옆에서 응원해준 동생 지수와 장모님, 장인어른께도 감사말씀 드리고 싶습니다. 어쩌면 저보다 저를 더 잘아는 사랑하는 아내 김의경과 딸 아영이의 지지는 박사학위를 받는데 결정적이었습니다. 부모님과 아내, 딸에게 이 논문을 바칩니다. 일일히 언급못했지만 부족한 저에게 도움을 주신 모든 분들께 정말

감사합니다.